Dissociative electron attachment and vibrational excitation of H_2 by low-energy electrons: Calculations based on an improved nonlocal resonance model. II. Vibrational excitation

J. Horáček,* M. Čížek, K. Houfek, and P. Kolorenč
Charles University, Faculty of Mathematics and Physics, Prague, Czech Republic

W. Domcke
Department of Chemistry, Technische Universität München, Germany

We treat vibrational excitation of hydrogen by low-energy electrons using an improved nonlocal resonance model. The model is based on accurate *ab initio* data for the $^2\Sigma_u^+$ shape resonance and takes full account of the nonlocality of the effective potential for nuclear motion. Integral vibrational excitation cross sections were calculated for numerous initial and final rovibrational states of the hydrogen molecule, and the dependence of the vibrational excitation cross section on the rovibrational initial target state has been investigated. The vibrational excitation cross sections are in very good agreement with measurements for the transitions $v=0 \rightarrow 1$ and $v=0 \rightarrow 2$, while for higher vibrational channels the agreement is less satisfactory. However, the oscillatory structures in $v=0 \rightarrow 4$ vibrational excitation and higher channels predicted by Domcke and collaborators and measured by Allan are described by the present calculation, in very good agreement with the experimental data. A detailed analysis of the origin of the oscillations has been performed. It is shown that the oscillations can be qualitatively understood within the so-called boomerang model of Herzenberg. The resonance contribution to the vibrationally elastic scattering ($v \rightarrow v$) is also discussed. It is found that this cross section is dominated at low energies by the resonance contribution, as predicted by Schulz. The calculated integral vibrational excitation cross sections generally are in good agreement with other theoretical data obtained by different approaches. A comprehensive study of the effect of isotopic substitution has been performed, and an inverse isotope effect in vibrational excitation has been found for certain vibrational levels of the target.

DOI: 10.1103/PhysRevA.73.022701   PACS number(s): 34.80.Ht

I. INTRODUCTION

The first observation of the vibrational excitation (VE) of molecular hydrogen was reported in 1931 by Ramien [1], but was widely disbelieved because the measured cross section was considered too large and no simple explanation could be found at that time [2]. Subsequent experiments of Schulz [3], Engelhart and Phelps [4], and Ehrhardt *et al.* [5] confirmed the large cross sections. The large magnitude of the VE cross section was explained in terms of a resonance model by Bardsley, Herzenberg, and Mandl invoking the $^2\Sigma_u^+$ state of H_2^- [6,7]. Excitation cross sections to higher final channels ($v=0 \rightarrow 1$, 2, 3, and 4) were measured, among others, by Ehrhardt *et al.* [5], Linder and Schmidt [8], and Allan [9] up to $v=6$. To the best of our knowledge, there exists only one rotationally resolved measurement of electron hydrogen elastic scattering performed by Linder and Schmidt in 1971 [8]. Vibrational excitation of D_2 was discussed by Buckman and Phelps [10]. In this context, it is worthwhile to mention the long-standing issue of the disagreement of VE cross sections measured by beam and swarm methods [10–12]. The results sometimes differ by as much as 60%.

The electron-H_2 collision system, being the most fundamental of all electron-diatomic-molecule scattering systems, has been the subject of numerous theoretical studies.

Electron-molecule scattering theory prior to 1980 was reviewed by Lane [13]. For a more recent review, see, e.g., Morrison [14]. From recent works we mention the calculations based on the frame-transformation theory by Robicheaux [15] and Gao [16], the nonlocal resonance theory of Bardsley and Wadehra [17], the *ab initio* calculation of Rescigno *et al.* [12], the semiclassical approach of Kazansky and Yelets [18,19], the nonadiabatic phase matrix method of Mazevet *et al.* [20,21], the body-frame vibrational close coupling approach of Lee and Mazon [22], and the Faddeev equation approach by Pozdneev [23]. All calculations presented in this paper are based on the improved nonlocal resonance model developed by Čížek, Horáček, and Domcke [24]. The process of dissociative attachment (DA) has in detail been studied in the first part of this paper [25] which we will cite in the following text as paper I.

The input data for the nonlocal resonance model [26] for a diatomic target molecule are represented by the three functions $V_0(R)$, $V_d(R)$, and $V_{d\varepsilon}(R)$. The target potential-energy function $V_0(R)$ can directly be obtained from *ab initio* calculations. The discrete state potential $V_d(R)$ and its coupling to the continuum $V_{d\varepsilon}(R)$ representing the H_2^- resonance (at short internuclear distance) and the H_2^- bound state (at intermediate and large internuclear distances) have been obtained by *ab initio* calculations based on many-body Green's function methods and the projection operator formalism [27,28]. The potential function $V_d(R)$ for large R [24] has been recovered from accurate *ab initio* calculations [29] of the H_2^-

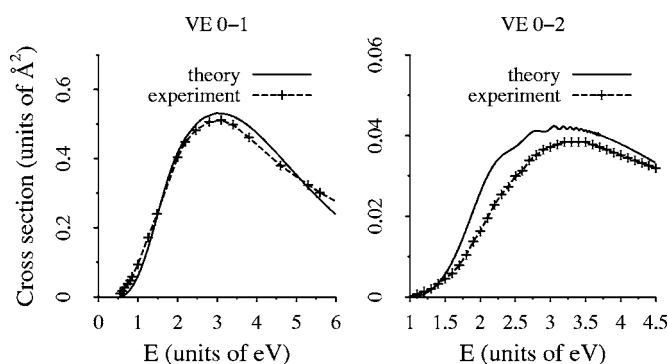*Electronic address: horacek@mbox.troja.mff.cuni.cz

FIG. 1. Left panel: calculated integral $0 \rightarrow 1$ VE cross section (solid line) compared with the measurement of Ehrhardt *et al.* [5] (crosses). Right panel: calculated integral $0 \rightarrow 2$ VE cross section compared with the measurement of Allan [9].

potential energy function. All parameters of the model are thus determined by *ab initio* calculations. A full description of the model is given in the Appendix of paper I.

II. RESULTS

In this section we will discuss our calculated integral VE cross sections for various initial states of the target molecules. Let us start with the ground vibrational state $v=0$. The methods employed for the treatment of the nuclear dynamics of H_2^- and the calculation of the cross sections are described in paper I as well as in previous publications [24,28].

A. Low final channels

It is well known (see, e.g., [9]) that the cross sections for $v=0 \rightarrow 1$ and $v=0 \rightarrow 2$ VE transitions of molecular hydrogen are smooth functions of the electron energy without any apparent structure. For higher final vibrational channels $v=0 \rightarrow 3, 4, 5, 6$, however, oscillatory structures converging to the threshold of DA appear. These oscillations were predicted by Mündel, Berman, and Domcke [28] and confirmed soon experimentally by Allan [9]. We will discuss the origin of the oscillations in a later section.

The calculated $0 \rightarrow 1$ integral VE cross section is shown in Fig. 1 (left panel) in comparison with the experimental cross section measured by Ehrhardt *et al.* [5]. The agreement between experiment and theory is very good up to 6.0 eV collision energy. A similar degree of agreement is found also for $0 \rightarrow 2$ VE (right panel of Fig. 1).

The present $0 \rightarrow 1$ VE cross section also agrees very well with the majority of other calculations. This is demonstrated in Fig. 2. In this figure, the present results are compared with the result of Bardsley and Wadehra [17,30] obtained with the local-complex-potential model, the result of Mazevet *et al.* [20], obtained by a body-frame vibrational close-coupling (BFVCC) calculation, and the results of Robicheaux, obtained with the frame transformation method [15]. All calculations agree qualitatively with the present results and with the experiment of Ehrhardt *et al.* [5] with the exception of the empirical local-complex-potential model (this model was
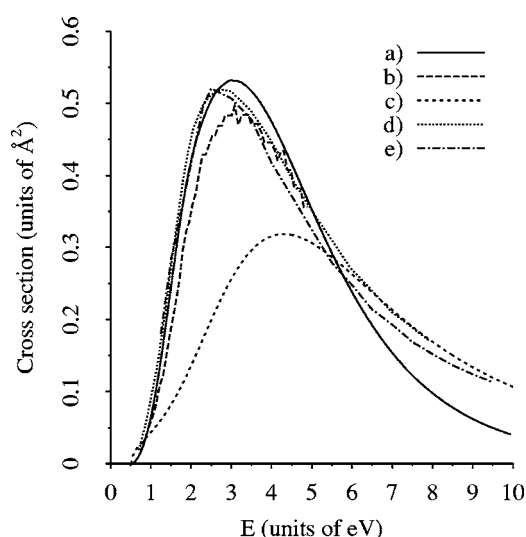

FIG. 2. Calculated integral $0 \rightarrow 1$ VE cross section (solid line) compared with other calculations: (a) present results, (b) body-frame transformation theory of Robicheaux [15], (c) nonlocal model of Bardsley and Wadehra [30], (d) BFVCC data of Mazevet *et al.* [20], and (e) close-coupling calculation of Lee and Mazon [22].

defined to fit the experimental dissociative attachment cross sections), which gives a too small cross section at low energies (but agrees with the experimental as well as other theoretical data at energies above 7.0 eV). At higher energies, the present $0 \rightarrow 1$ cross section is too low compared with experiment [5] and the close-coupling and frame-transformation calculations. This is not unexpected, since the present nonlocal resonance model includes only the lowest-energy $(^2\Sigma_u^+)$ shape resonance.

The results given above were obtained for molecules in the ground rotational state $J=0$. The effect of target rotation on the VE cross section—i.e., the dependence of the $0 \rightarrow 1$ VE cross section on the rotational quantum number J—is
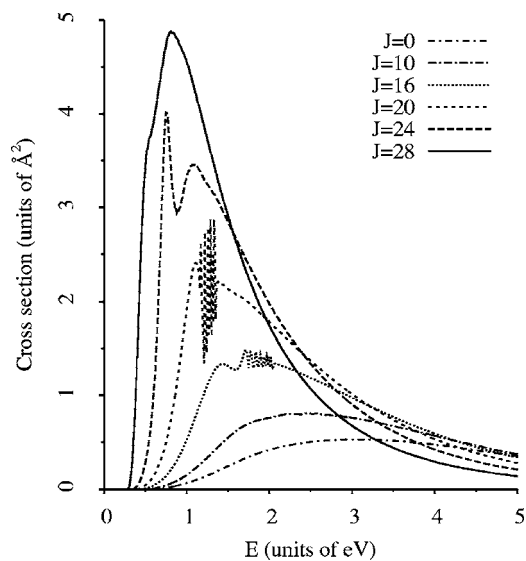

FIG. 3. Integral $v=0 \rightarrow 1$ VE cross sections for various rotational states J.
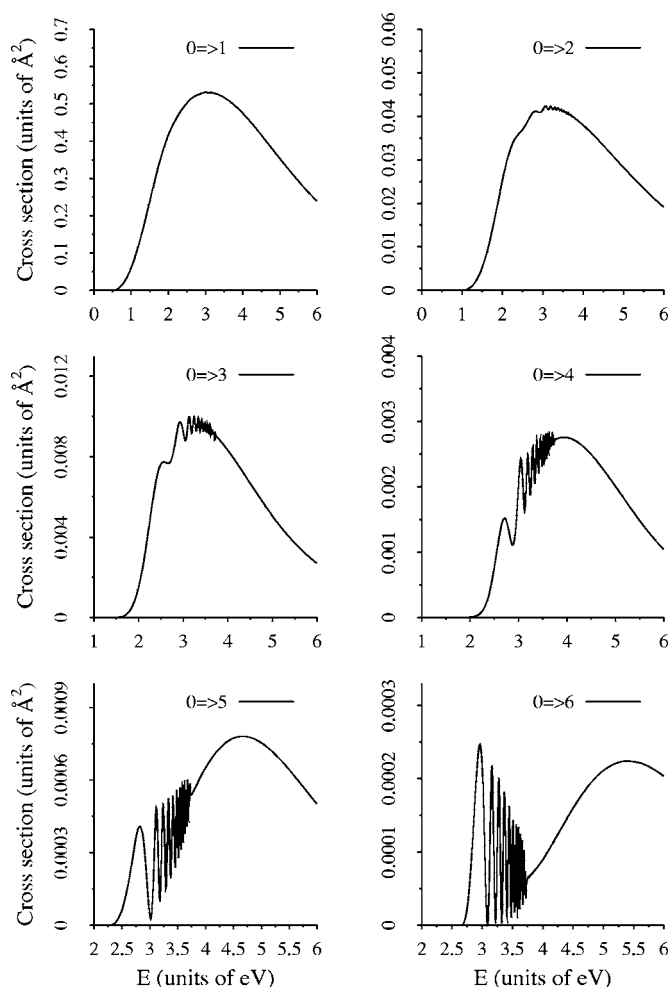
FIG. 4. Calculated integral VE cross sections of H_2 from the ground rovibrational state.

FIG. 5. Oscillations in the $0 \rightarrow 4$ VE cross section of H_2 below the DA threshold calculated at the temperature $T = 300$ K (solid line) compared with the experimental data of Allan [9] (crosses).

shown in Fig. 3. The magnitude of the VE cross section increases with increasing J, and oscillatory structures become more visible for $J > 10$. These structures disappear again for large J ($J \geqslant 24$), because the thresholds of dissociative attachment for molecules in such high rotational states lie too low (these structures appear below this threshold, as discussed later). The change of the cross section shape with J is a consequence of the change of the potential shapes. Qualitatively speaking, we can think of a centrifugal force which pushes the atomic constituents apart. The resonance position moves towards lower energies, since the average position $\langle R \rangle$ in $v = 0$ state increases with increasing J. The energy difference of the potentials $V_0(R)$ and $V_d(R)$ decreases with R as does the width of the resonance.

B. Higher final channels

The calculated integral VE cross sections from the rovibrational ground state up to $v = 6$ are shown in Fig. 4. The $v = 0 \rightarrow 3$ cross section was measured by Ehrhardt *et al.* [5] and the measurements were extended to $v = 0 \rightarrow 4$-6 channels by Allan [9]. In contrast to the lowest two channels, our calculation overestimates the measured cross section by fac-
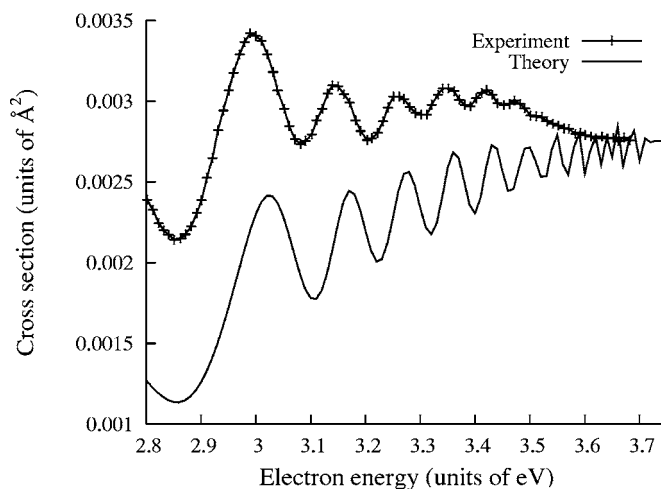
tor of 2–3 for the $v = 0 \rightarrow 3$-6 channels. The origin of this discrepancy is unknown.

Unlike the magnitude of the cross sections, their shape is in good agreement with the experiments. It is seen that tiny oscillating structures show up in the $v = 0 \rightarrow 2$ channel, which gradually become more intense for higher vibrational channels. The same behavior is seen in the experiment of Allan [9]. This is demonstrated in Fig. 5, where the calculated oscillatory structures below the opening of the DA channel in the $0 \rightarrow 4$ VE channel at a gas temperature of $T = 300$ K are compared with the experimental data of Allan [9]. Since the experimental data are relative, we rescaled them so that the experimental curve and the calculated cross section coincide at the DA threshold (the original data, normalized to a measurement of Ehrhadt *et al.* [5] in lower channels, were larger by more than a factor of 2). At least seven discrete peaks can be discerned in the experimental cross section. No peaks are visible in the experimental data above 3.5 eV. The agreement between the positions and widths of the calculated peaks is very good; only a small systematic shift of 20–30 meV is observed. The calculated cross section has a tendency to rise, whereas the experimental one is more or less oscillating around a constant value. The reason for this discrepancy is unknown to us, but generally the cross sections in the vicinity of thresholds for the opening of new channels are very sensitive functions of model parameters and small parameter changes may lead to significant changes of the cross sections. For example, the $\pm 10\%$ change in the magnitude of the coupling $V_{d\epsilon}(R)$ can shift the phase of the oscillations by π and change the overall magnitude of the $0 \rightarrow 4$ VE cross section by a factor of 2 in this energy region.

To shed more light on the character of the oscillatory structures, we plotted the cross sections close to the DA threshold for all $v = 0 \rightarrow 0$-6 channels in a single figure; see Fig. 6. A smooth background (see the figure caption) was subtracted from each curve, and the result was shifted for better visibility of the structures. We observe that the structures are present even in the lowest VE channels, where they are obscured by the large unstructured cross section. The
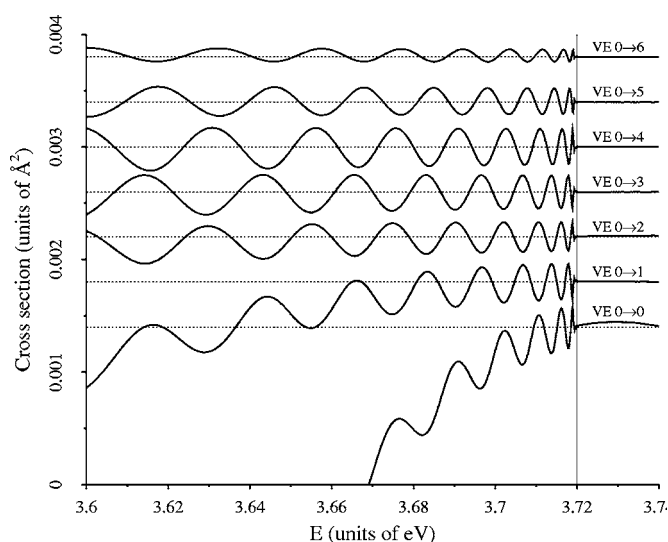
FIG. 6. VE cross sections in the vicinity of the DA threshold (vertical line). A smooth background (given by linear approximation of the energy dependence of the cross section in the range $E = 3.72$–3.74 eV) was subtracted from each curve, and the results are vertically displaced for better visibility of the oscillations.
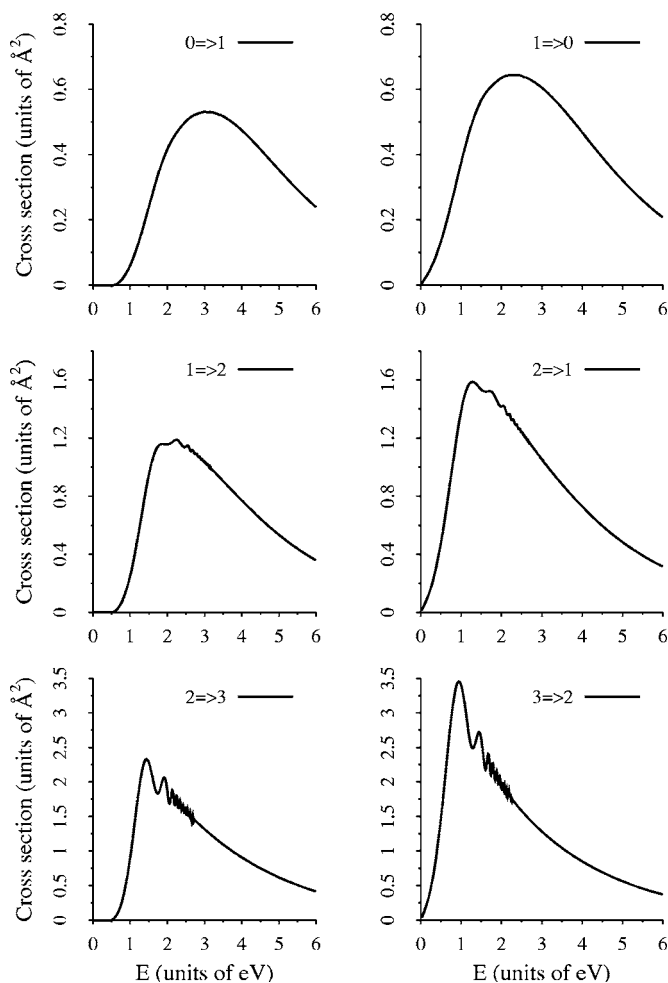

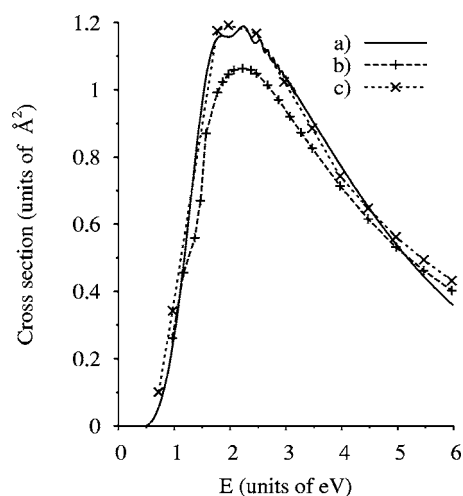FIG. 7. Comparison of $v \to v+1$ excitation and $v+1 \to v$ deexcitation cross sections for $v=0$–2.

FIG. 8. $1 \to 2$ VE cross sections compared with the calculation of Lee and Mazon [22]: (a) present calculation, (b) configuration-interaction calculation of Lee and Mazon, and (c) HF calculation of Lee and Mazon.

basic properties of the oscillations are (i) a narrowing of the oscillations towards the dissociative attachment threshold, (ii) amplitude inversion between subsequent channels, and (iii) the magnitude of the oscillations similar in all channels.

C. Vibrationally excited targets

So far, we discussed the process of vibrational excitation from the ground vibrational state $v=0$ of the target molecule. Considering vibrationally excited target molecules, we can study in addition to vibrational excitation also the process of vibrational deexcitation, $v \to v-1$, $v-2$, etc., which plays an important role in plasma modeling. Moreover, the cross sections for vibrationally excited molecules display features which are absent in the excitation from the vibrationally ground state.

As discussed above, no oscillatory structures are apparent in the $v=0 \to 1$, $J=0 \to 0$ VE cross section. If the target molecule is vibrationally excited, oscillatory structures appear even for excitation of one vibrational quantum. In Fig. 7, the calculated cross sections for $v \to v+1$ excitation and $v \to v-1$ deexcitation are shown. It is seen that the magnitude of the VE cross section increases and the profile narrows with increasing v. At present, there are no experimental data available for scattering on excited molecules. Recently, however, Lee and Mazon have calculated the VE cross section for vibrationally excited H_2 using the body-frame vibrational close-coupling approach [22]. It is thus possible to compare the results of the present resonance theory for excited molecules with the results of the close-coupling calculation which does not explicitly invoke a resonance (of course, the resonance is implicitly present).

In Fig. 8 the present results are compared with the calculation of Lee and Mazon [22]. They have reported two variants of the calculation: one based on the Hartree-Fock description of H_2 (denoted by HF in the figure), the other based on the configuration interaction (CI) description of H_2. The agreement between the resonant and nonresonant *ab initio*

theories is remarkably good. The present nonlocal resonance model is based on the very precise calculation of Senekowitsch *et al.* [29] of the hydrogen-anion potential-energy curve. This calculation was carried out with the multireference CI method, taking into account all singly and doubly excited configurations. The reason why our data agree better with the less-accurate HF calculation of Lee and Mazon than the CI calculation is unknown to us.

D. Interpretation of the oscillations

The properties of the oscillatory structures appearing in the VE cross sections below the DA threshold can fully be explained within the so-called boomerang model (see Herzenberg and Mandl [31] and Herzenberg [32]) which has been proposed for the interpretation of similar, but more pronounced, oscillations observed in VE cross sections of $e^- + N_2$ collisions [33].

According to the boomerang model, the oscillations can be understood as a consequence of the interference of two processes. The first one is the fast direct decay of the intermediate anion (broad shape resonance) in the autodetachment region with little change in the molecular geometry (this process determines the overall envelope of the cross section). The second process is the motion of the nuclei away from the autodetachment region (extension of the internuclear distance R) until the attractive part of the potential $V_d(R)$ inverts their motion, sending them back into autodetachment region, where the molecular anion quickly decays by releasing an electron. In the $e^- + H_2$ system, the second process is allowed only in a relatively narrow energy interval below the DA threshold, which explains appearance of the oscillations in the VE cross section right below this threshold. The magnitude of the oscillations is given by the relative amplitudes of the two interfering processes, while the positions of the maxima and minima are determined by the relative phase of the wave functions corresponding to the two processes at different energies (see below). In the following, we will explain in detail all features of the oscillatory structures, using the ideas of the boomerang model which is based on the local-complex-potential approximation. To get correct quantitative results (especially the magnitude of oscillations relative to the overall envelope) one has to take full account of nonlocal effects.

If we compare oscillations in different VE cross sections, we find that the magnitude of the oscillations near the DA threshold is almost the same in VE cross sections from the same initial vibrational state v_i to different final states v_f, but is rapidly growing when the vibrational quantum number v_i of the initial state is increasing. The former behavior was illustrated in Fig. 6, where VE cross sections $0 \rightarrow 0$–6 for energies near the DA threshold were shown. The latter effect can be observed in Fig. 7 as well as in Fig. 15 (to be discussed below). We can explain both behaviors qualitatively if we realize that the magnitude of the oscillations is proportional to the amplitude of the reflected wave and that this amplitude depends strongly on the initial vibrational state, but not at all on the final one. The kinetic energy of the nuclear motion of the molecule in a higher initial vibrational
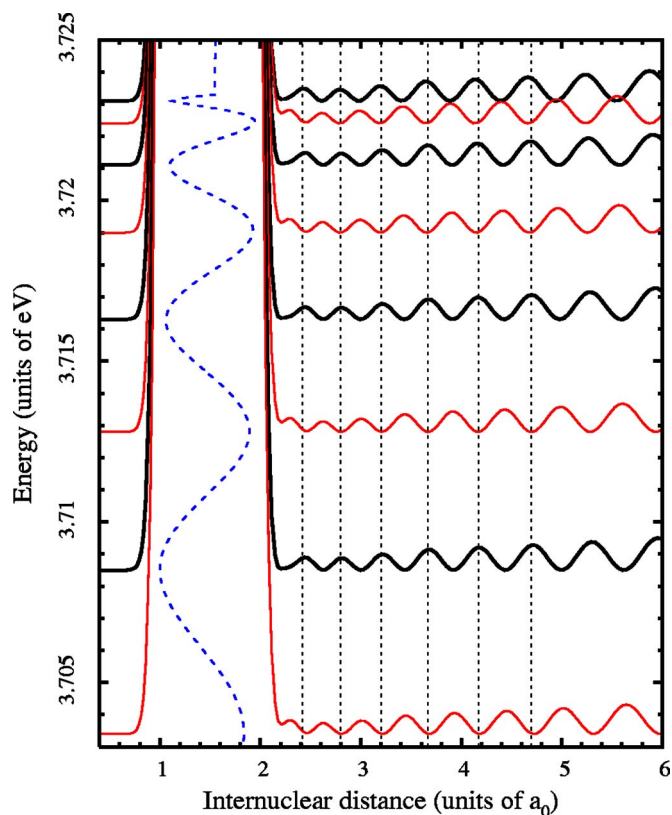

FIG. 9. (Color online) Time-independent wave functions [solutions of Eq. (7) of paper I] of the nuclear dynamics for the initial rovibrational state $v_i = 0$, $J = 0$ at several energies right below the DA threshold. All wave functions exhibit a huge peak centered at the equilibrium internuclear distance of the neutral molecule (corresponding to the directly decaying wave) and a tail at larger internuclear distances (corresponding to the reflected wave). All tails of the wave functions at energies where the VE cross section $0 \rightarrow 3$ (shown by the dashed line) has maxima (solid curves) *or* minima (long-dashed curves) are *in phase*.

state is larger and consequently it is more probable for the molecular anion to leave the autodetachment region before it releases an electron. The amplitude of the reflected wave will therefore be larger relative to the amplitude of the directly decaying wave.

It is noteworthy to mention here the connection between the magnitude of the oscillations in the VE cross section and the magnitude of the DA cross section near the threshold. The amplitude of the reflected nuclear wave functions right below the DA threshold is almost energy independent (see Fig. 9) and is comparable to the amplitude of the outgoing waves in the DA channel near the threshold. We can thus conclude that the magnitude of the oscillations will be proportional to the DA cross section near the threshold for the same initial state. This is actually observed in H_2 when increasing the rotational or vibrational quantum number of the initial state (both the magnitude of the oscillations and the DA cross section are rapidly increasing).

Other important features of the oscillations are their narrowing with increasing electron energy towards the DA threshold and the amplitude inversion (first observed in $e^- + N_2$; for details, see [32]) which means that if the VE cross

TABLE I. Ratio of $0 \to 1$ VE cross sections for HD and D_2 molecules to that for H_2 molecules. Theory: Atems and Wadehra [38]. Peaks: the value at the peak of the calculated cross sections (i.e., at different electron energies). 4 eV: ratios taken at the energy 4.0 eV. 5 eV: the same at 5.0 eV. Expt. (a): $v=0 \to 1$, $J=0 \to 0$ cross sections as measured by Chang and Wong [37]. Expt. (b): $v=0 \to 1$, $J=0 \to 2$ cross sections [37].

	Theory [38]	Peaks	4 eV	5 eV	Expt. (a)	Expt. (b)
HD/H_2	0.866	0.87	0.88	0.89		
D_2/H_2	0.707	0.71	0.74	0.76	0.55	0.72

section in a given vibrational channel, $v_i \to v_f$, has a maximum at energy E, then the vibrational excitation cross section to the next higher channel, $v_i \to v_f+1$, has a dip at almost the same energy (see Fig. 6).

The narrowing of the oscillations is related to the relative phases of the reflected waves for different energies. Qualitatively speaking, the wave with energy approaching the DA threshold has to travel farther and farther in the long-range part of the potential $V_d(R)$. The energy difference of two waves which will be reflected with the same relative phase is decreasing towards the DA threshold, similarly as the energy distance of two bound states in the long-range potential. An illustration of this behavior in terms of time-independent wave functions is shown in Fig. 9 where we have plotted the squares of wave functions at energies corresponding to maxima (solid curves) or minima (long-dashed curves) of the oscillations in the $0 \to 3$ VE cross section near the DA threshold (short-dashed curve). One can clearly see (take the auxiliary vertical lines as a guide) how the relative phase of the wave functions is related to the oscillatory structure.

Finally, the amplitude inversion appears as a consequence of the overlap of the reflected wave function (the same for all final states) with the different final molecular vibrational wave functions. Qualitatively, if the vibrational state v_f is *in phase* with the reflected wave at a given energy (maximum in the VE cross section), then the vibrational state v_f+1 is almost *out of phase* with that reflected wave [where one vibrational state v_f has nodes, the subsequent one has maxima or minima (not exactly at the same place, but very close)].

Recently, the oscillatory structures in $e^- + H_2$ collisions were discussed by Narevicius and Moiseyev [34,35] as numerous overlapping resonances in a local complex potential. Although this interpretation in principle is mathematically correct, it does not give a satisfactory physical description of the process. This is seen from Fig. 9, where the wave function does not show any strong energy dependences (typical for resonant behavior). We note here that for high rotational quantum numbers J an inner barrier, through which the system can tunnel and which prevents the system from returning to the autodetachment region, will appear in the effective potential due to the centrifugal term. Consequently the molecular anion can exist for a very long time, leading to very narrow resonances in the VE cross sections. Then the interpretation in terms of long-lived metastable states is more appropriate. In principle, there is smooth transition between the two cases. Such long-lived states were experimentally observed recently by Golser *et al.* [36] and will be discussed within the present model in more detail in a separate paper.

III. ISOTOPE EFFECT IN VIBRATIONAL EXCITATION

The study of isotope effects in vibrational excitation has not received much attention. To the best of our knowledge, only two papers have addressed this problem from the point of theory. Chang and Wong [37] have employed frame-transformation theory to study the isotope effect in molecular hydrogen. Later Atems and Wadehra [38] used the local-complex-potential approach to propose an approximate theory of the isotope effect in VE in hydrogen halides. According to this theory, the ratio of the VE cross sections for DX and HX molecules, where $X=$F, Cl, Br, is independent of the energy and depends only on the initial and final vibrational states v_i and v_f as well as on the reduced mass μ:

$$\frac{\sigma(DX)}{\sigma(HX)} \approx \left(\frac{\mu_{DX}}{\mu_{HX}}\right)^{-|v_i-v_f|/2}. \tag{1}$$

This theory was applied also to molecular hydrogen and predicts, for example, that the $0 \to 1$ VE cross section of D_2 is smaller by a factor of $1/\sqrt{2} \sim 0.71$ than that of H_2. According to [38], the scaling law, Eq. (1), is accurate with an error less than 35%. According to the scaling law, Eq. (1), the $0 \to 1$ VE cross section in HD is thus smaller by a factor of 0.87 of that of H_2. As predicted by the theory [38], the isotope effect is more pronounced as v_f increases. The ratios ρ of the calculated $0 \to 1$ cross sections at several energies are shown for $J=0$ in Table I. The values in the second column ("peaks") were obtained as the ratio of the peak values of the respective cross sections—i.e., not at the same energy. The other data were calculated for the same energy, 4.0 eV and 5.0 eV, respectively, for the ground rotational state.

Two experimental data are available [37]: for the purely rotationally elastic $v=0 \to 1$ transition at the temperature $T=300$ K, $\rho=0.55$, and for simultaneous vibrational and rotational excitation, $v=0 \to 1$, $J=0 \to 2$, $\rho=0.72$. In an analysis performed by Chang and Wong [37] at a nonzero temperature T, two isotope effects are in fact seen: One, due to the change of the reduced mass, is that all cross sections behave as indicated in Eq. (1); the other enters via the changes in the rotational-state populations (different nuclear spin statistics and rotational constants). If this is taken into account, the theory of Chang and Wong [37] agrees very well with the experiment. For example, the predicted ratio for the $v=0 \to 1$, $\Delta J=0$ transition at 4.0 eV is 0.56 whereas the experimental value is 0.55 [37]. For the transition $v=0 \to 1$, $J=0 \to 2$ the theory yields the value 0.71 and the experiment 0.72. The latter value is in very good agreement with the present calculation, which yields the value 0.71 for the ratio of the
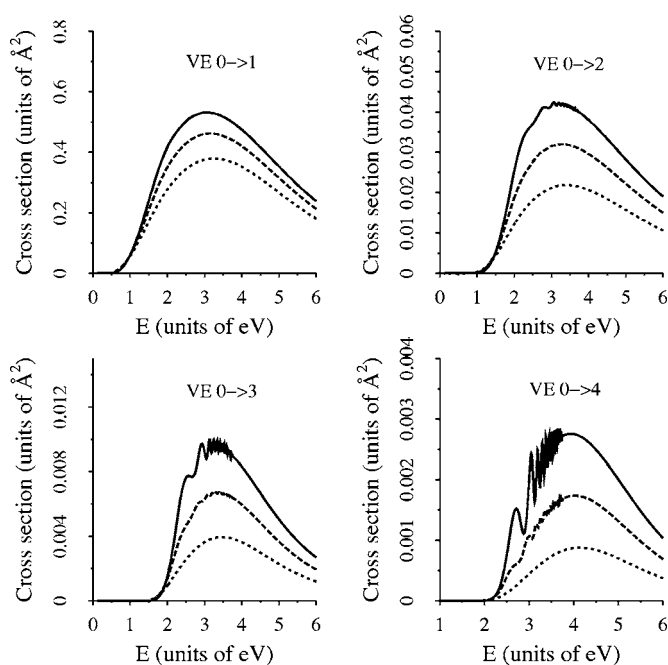
FIG. 10. Isotope effect in vibrational excitation: calculated integral $0 \to 1, 2, \ldots, 4$ VE cross sections for H_2 (solid line), HD (long-dashed line), and D_2 (short-dashed line).
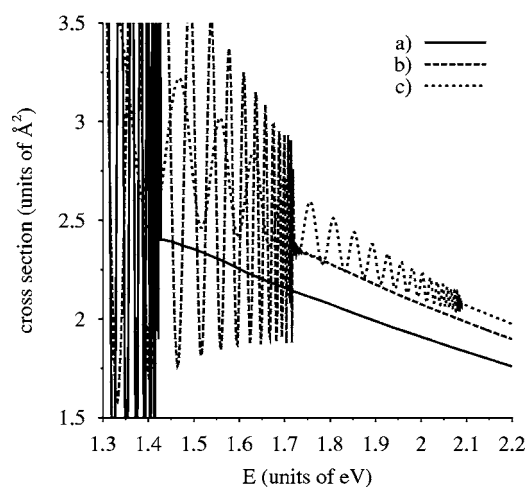

FIG. 11. Cross sections for the $5 \to 6$ transition in H_2, HD, and D_2 in the region of the dissociative attachment threshold: (a) H_2, (b) HD, and (c) D_2. Note that the VE cross section of D_2 is the largest of all cross sections in this energy range.

peaks and 0.74 for the ratio at $E = 4.0$ eV; see Table I. According to the theory [38], the scaling factor of Eq. (1) is energy independent, provided the energy is high enough. The present calculation shows that the ratios are approximately constant only at energies above about 4.0 eV.

VE cross sections for the transitions $v = 0 \to v = 1, 2, 3, 4$ and $J = 0$ are shown in Fig. 10. As predicted by Eq. (1), the isotope effect is more pronounced as the final vibrational quantum number v_f increases.

To see how the isotope effect for excitation by one vibrational quantum number, $v \to v+1$, evolves with increasing v we calculated the cross sections for H_2, HD, and D_2 molecules and the transitions $0 \to 1, \ldots, 5 \to 6$. According to the scaling law [38], the ratio of the cross sections should be constant. The calculated cross sections are collected in Table II. The ratio of the cross sections increases with increasing initial vibrational state v both for HD as well as for D_2. For the $5 \to 6$ transition, the calculated D_2 cross section exceeds that for H_2 by a factor of 1.07.

In Fig. 11, we plot the VE cross sections for the $5 \to 6$ transition in the energy region of the dissociative attachment threshold. Clearly, the D_2 cross section is the largest and also the cross section for HD is larger than the H_2 cross section; i.e., we observe an inverse isotope effect. This effect is more pronounced in hydrogen halides [39].

Another interesting aspect is the scaling of the amplitude of the oscillations in the VE cross sections below the DA threshold with reduced nuclear mass. The present calculations indicate that the magnitudes of the oscillations exhibit a huge isotope effect, the H_2/D_2 magnitude ratio being about 50. In Fig. 12, we show the $0 \to 4$ VE cross section of H_2 in the region of the oscillations compared with the cross sections of HD and D_2. To reveal the isotope effect in the oscillations, we substracted the overall mass dependence in accordance with the scaling law of [38] by multiplying the HD cross section by a factor of 2 and that of D_2 by a factor of 4. It is seen that overall dependence of the cross sections follows the scaling law, Eq. (1) (on average all three cross sections are of similar shape), but the magnitude of the oscillation changes significantly from H_2 to HD and D_2. This finding is in agreement with our reasoning given in Sec. II D.

TABLE II. $v \to v+1$ VE cross sections for H_2, HD, and D_2 molecules and their ratio to H_2 cross sections. Note that for the transition $v = 5 \to 6$, the D_2 cross section exceeds that for H_2 and HD. The cross section are in $Å^2$; the electron energy equals 4.0 eV.

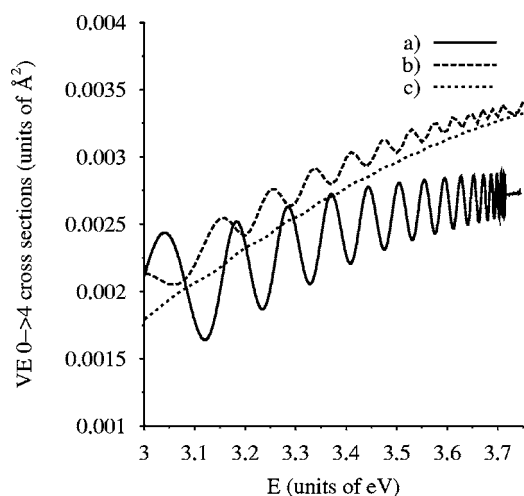| Transition	H_2	HD	HD/H_2	D_2	D_2/H_2	Theory [38] D_2/H_2
$0 \to 1$	0.475	0.420	0.88	0.352	0.74	0.71
$1 \to 2$	0.769	0.706	0.92	0.617	0.80	0.71
$2 \to 3$	0.908	0.864	0.95	0.788	0.87	0.71
$3 \to 4$	0.950	0.930	0.98	0.887	0.93	0.71
$4 \to 5$	0.939	0.948	1.01	0.933	0.99	0.71
$5 \to 6$	0.887	0.929	1.05	0.945	1.07	0.71

FIG. 12. Cross sections for the $v = 0 \rightarrow 4$ transition. (a) VE cross section of H_2 (solid line), (b) VE cross section of HD, multiplied by 2 (dashed line), and (c) VE cross section of D_2, multiplied by 4 (dotted line).

IV. SUMMARY

Cross sections for vibrational excitation of molecular hydrogen by low-energy electron impact were calculated with an improved nonlocal resonance model [24]. Cross sections for a large number of rovibrational initial target states were calculated with high-energy resolution and compared with existing experimental data and other theoretical data.

It was found that the degree of agreement with experiment ranges from excellent (for $0 \rightarrow 1$ and $0 \rightarrow 2$ VE) to moderate (for more inelastic channels). Our calculations predict an unexpected isotope effect which does not seem to have a classical analog: at the same collision energy the VE cross section of the heavier (deuterated) compound is larger than the cross section of the lighter (hydrogenated) compound. This phenomenon is observed when the initial target state is energetically close to the threshold of DA. The explanation of the inverse isotope effect in VE is not as simple as for DA. It seems that a strong coupling of DA and VE channels is responsible for this phenomenon, but other mechanisms may be involved. One may envisage, for example, that the lowering of the VE threshold for deuterated molecules may play a role. The magnitude of the cross section is very sensitive to the position of the threshold on the energy scale. Another feature that obviously plays a role is that for vibrationally or rotationally excited molecules the range of accessible internuclear distances is larger than that of ground-state molecules. The particles probe different regions and are influenced by different interactions. In our understanding, the inverse isotope effect is a complex combination of several mechanisms.

The absolute magnitude of the oscillations in VE $v_i \rightarrow v_f$ cross sections was found to be insensitive to the final state v_f, but rather sensitive to v_i, in a qualitatively similar way as the DA cross section. The behavior of the oscillations (including the isotope effect) can qualitatively be understood within the boomerang model.

In conclusion, the present nonlocal resonance model gives a reasonably accurate description of the essential features of electron-hydrogen vibrational excitation for energies below 5.0 eV. Many of these cross sections (e.g., for high vibrational and/or rotational excitation) have not been measured. It is hoped that the data (which are available from the authors upon request) may prove useful for the modeling of electronic processes in hydrogen gas.

APPENDIX

Elastic scattering

The nonlocal resonance model was designed to treat resonant inelastic processes such as vibrational excitation and dissociative attachment. The direct (nonresonant) scattering contribution to these processes is generally small and can be neglected to a good approximation. In the case of elastic scattering, however, the direct part is usually dominant and cannot be neglected. Nevertheless, it is meaningful to study the elastic scattering in terms of the nonlocal resonance model. First of all, the direct (nonresonance) elastic scattering cross section is a smooth function of energy in the energy range considered. The calculated resonant scattering cross sections, on the other hand, exhibit narrow oscillatory struc-
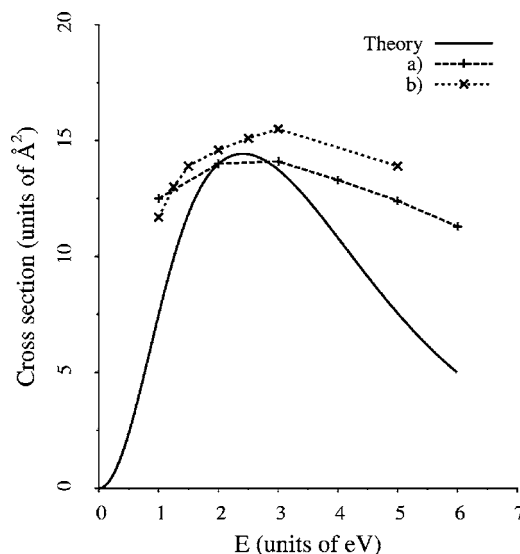

FIG. 13. Calculated resonant contribution to the integral elastic electron scattering for the ground rovibrational state of the hydrogen molecule (solid line). Experimental data: (a) rotationally resolved measurement of Linder and Schmidt [8] and (b) measurement of Brunger and Buckman [41].
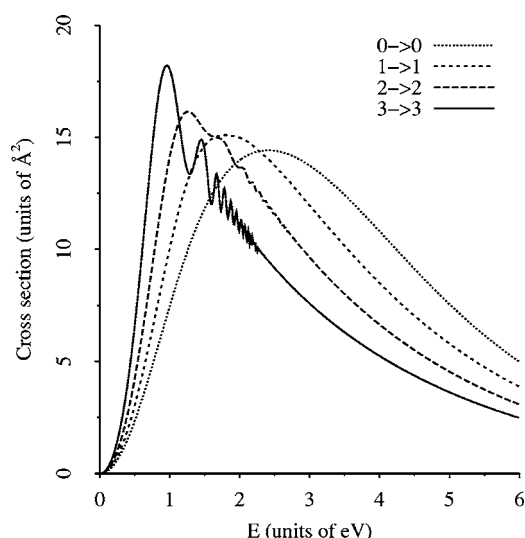
FIG. 14. Calculated resonant contribution to the elastic scattering cross section of H_2 for the vibrational states $v=0$–3 of the target molecule.
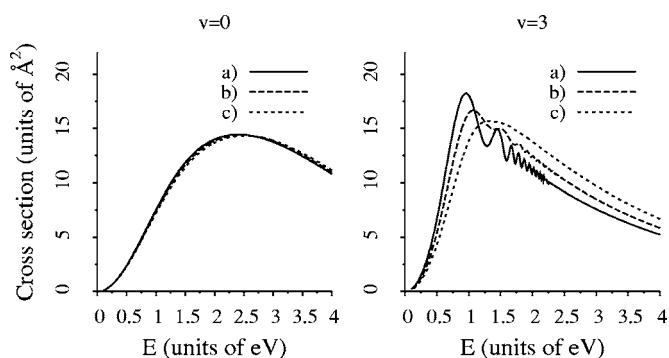

FIG. 15. Isotope effect in the resonant part of the elastic scattering cross sections: (a) H_2, (b) HD, and (c) D_2, for the ground rotational and vibrational state (left panel) and for vibrationally excited molecules, $v=3$ (right panel).

tures which should be present in the total scattering cross section and might be observed experimentally [40]. Second, the nonlocal resonance model can be used to study the isotope effect in elastic as well as vibrational excitation cross sections.

In the present approach, only the $^2\Sigma_u^+$ resonance contribution to the total cross section can be obtained. The calculated resonant vibrationally elastic scattering cross section is plotted in Fig. 13 together with two experimental data: (a) the rotationally resolved integral elastic scattering cross section of Linder and Schmidt [8] and (b) the integral elastic scattering cross section of Brunger and Buckman [41]. It is seen that in the energy range 2–3 eV the resonance cross section dominates the total elastic cross section. This confirms the conjecture of Schultz and Asundi [42] that the peak in the elastic cross section at 2 eV has its origin in the $^2\Sigma_u^+$ resonance.

The shape of the resonance contribution of the elastic cross section depends on the initial vibrational state of the target. In Fig. 14, the calculated resonance contributions ($v=i\to i$, $J=0\to 0$ transitions) are plotted for molecules in the initial vibrational states $v=0$–3. These cross sections are quite large, about 15 Å^2. The peak shifts to lower energies with increasing v, and the width decreases rapidly with increasing initial vibrational state of the molecule; the width [full width at half maximum (FWHM)] changes from almost 5.0 eV for the $0\to 0$ transition to about 2.0 eV for the

$3\to 3$ transition. This behavior can be understood as a shift of a universal curve towards lower energies, where it is cut off by the threshold, consistently with the different initial vibrational energy of the molecule. While the low-v cross sections are smooth functions of energy, oscillatory structures appear in the cross sections with increasing v_i. It is now experimentally possible to produce hydrogen molecules in highly rotationally and vibrationally excited states ($v\sim 10$, $J\sim 17$) [43–48] and these structures might therefore be observed. These features may possibly be used as a diagnostic tool for the detection of rovibrationally excited hydrogen molecules. The dependence of the magnitude of oscillations on the initial target state has been discussed in Sec. II D.

Isotope effect in elastic scattering

Isotopic substitution of H by D or T has a large effect on the process of dissociative attachment; see paper I. Here we briefly mention how isotopic substitution affects the cross sections of elastic scattering. For ground vibrational states, the resonance elastic scattering cross sections display a negligible isotope effect. This is demonstrated in Fig. 15, left panel, where the resonance elastic scattering cross sections are plotted for three isotopes: H_2, HD, and D_2. The role of the isotope effect increases, however, with increasing initial vibrational state of the target. In Fig. 15, right panel, we plot the resonance contribution to the elastic scattering cross section for all three isotopes for a vibrationally excited target, $v=3$. The shape of the VE elastic cross section now shows a stronger dependence on the nuclear mass. This is partly caused by a shift of the respective vibrational-state energy.

[1] H. Ramien, Z. Phys. **70**, 353 (1931).

[2] G. J. Schulz, Rev. Mod. Phys. **45**, 423 (1973).

[3] G. J. Schulz, Phys. Rev. **135**, A988 (1964); **136**, A650 (1964).

[4] A. G. Engelhardt and A. V. Phelps, Phys. Rev. **131**, 2115 (1963).

[5] H. Ehrhardt, L. Langhans, and H. S. Taylor, Phys. Rev. **173**,

222 (1968).

[6] J. N. Bardsley, A. Herzenberg, and F. Mandl, Proc. Phys. Soc. London **89**, 305 (1966); **89**, 321 (1966).

[7] I. Eliezer, H. S. Taylor, and J. K. Williams, J. Chem. Phys. **47**, 2165 (1967).

[8] F. Linder and H. Schmidt, Z. Naturforsch. A **26**, 1603 (1971).

[9] M. Allan, J. Phys. B **18**, 451 (1985).

[10] S. J. Buckman and A. V. Phelps, J. Chem. Phys. **82**, 4999 (1985).

[11] S. J. Buckman, M. J. Brunger, D. S. Newman, G. Snitchler, S. Alston, D. W. Norcross, M. A. Morrison, B. C. Saha, G. Danby, and W. K. Trail, Phys. Rev. Lett. **65**, 3253 (1990).

[12] T. N. Rescigno, B. K. Elza, and B. H. Lengsfield, J. Phys. B **26**, L567 (1993).

[13] N. F. Lane, Rev. Mod. Phys. **52**, 29 (1980).

[14] M. A. Morrison, Adv. At. Mol. Phys. **24**, 51 (1988).

[15] F. Robicheaux, Phys. Rev. A **43**, 5946 (1991).

[16] H. Gao, Phys. Rev. A **45**, 6895 (1992).

[17] J. N. Bardsley and J. M. Wadehra, Phys. Rev. A **20**, 1398 (1979).

[18] A. K. Kazansky and I. S. Yelets, J. Phys. B **17**, 4767 (1984).

[19] A. K. Kazansky, J. Phys. B **29**, 4709 (1996).

[20] S. Mazevet, M. A. Morrison, and R. K. Nesbet, J. Phys. B **31**, 4437 (1998).

[21] S. Mazevet, M. A. Morrison, O. Boydstyn, and R. K. Nesbet, Phys. Rev. A **59**, 477 (1999).

[22] M.-T. Lee and K. T. Mazon, Phys. Rev. A **65**, 042720 (2002).

[23] S. A. Pozdneev, J. Exp. Theor. Phys. **90**, 30 (2000).

[24] M. Čížek, J. Horáček, and W. Domcke, J. Phys. B **31**, 2571 (1998).

[25] J. Horáček, M. Čížek, K. Houfek, P. Kolorenč, and W. Domcke, Phys. Rev. A **70**, 052712 (2004) (paper I).

[26] W. Domcke, Phys. Rep. **208**, 97 (1991).

[27] M. Berman, C. Mündel, and W. Domcke, Phys. Rev. A **31**, 641 (1985).

[28] C. Mündel, M. Berman, and W. Domcke, Phys. Rev. A **32**, 181 (1985).

[29] J. Senekowitsch, P. Rosmus, W. Domcke, and H.-J. Werner, Chem. Phys. Lett. **111**, 211 (1984).

[30] R. Celiberto (private communication).

[31] A. Herzenberg and F. Mandl, Proc. R. Soc. London, Ser. A **270**, 48 (1962).

[32] A. Herzenberg, J. Phys. B **1**, 548 (1968).

[33] G. J. Schulz, Phys. Rev. **125**, 229 (1962).

[34] E. Narevicius and N. Moiseyev, Phys. Rev. Lett. **81**, 2221 (1998).

[35] E. Narevicius and N. Moiseyev, Phys. Rev. Lett. **84**, 1681 (2000).

[36] R. Golser, H. Gnaser, W. Kutschera, A. Priller, P. Steier, A. Wallner, M. Čížek, J. Horáček, and W. Domcke, Phys. Rev. Lett. **94**, 223003 (2005).

[37] E. S. Chang and S.-F. Wong, Phys. Rev. Lett. **38**, 1327 (1977).

[38] D. E. Atems and J. M. Wadehra, Chem. Phys. Lett. **197**, 525 (1992).

[39] J. Horáček, M. Čížek, P. Kolorenč, and W. Domcke, Eur. Phys. J. D **35**, 225 (2005).

[40] M. Čížek, J. Horáček, M. Allan, and W. Domcke, Czech. J. Phys. **52**, 1057 (2002).

[41] M. J. Brunger and S. J. Buckman, Phys. Rep. **357**, 215 (2002).

[42] G. J. Schulz and R. K. Asundi, Phys. Rev. Lett. **15**, 946 (1965).

[43] R. I. Hall, I. Čadež, M. Landau, F. Pichou, and C. Scherman, Phys. Rev. Lett. **60**, 337 (1988).

[44] I. Čadež, R. I. Hall, M. Landau, F. Pichou, and C. Schermann, J. Phys. B **21**, 3271 (1988).

[45] D. Popovič, I. Čadež, M. Landau, F. Pichout, C. Schermann, and R. I. Hall, Meas. Sci. Technol. **1**, 1041 (1990).

[46] S. Gough, C. Schermann, F. Pichou, M. Landau, I. Čadež, and R. I. Hall, Astron. Astrophys. **305**, 687 (1996).

[47] I. Čadež, R. I. Hall, M. Landau, F. Pichou, and C. Scherman, J. Chem. Phys. **106**, 4745 (1997).

[48] P. Vanka, D. C. Schram, and R. Engeln, Chem. Phys. Lett. **400**, 196 (2004).